International Journal of Applied Mathematics in Control Engineering 7 (2024) 25-31

Contents lists available at YXpublications

International Journal of Applied Mathematics in Control Engineering

Journal homepage: http://www.ijamce.com

Efficiency Calculation of Solar Concentrator Field Based on Monte Carlo Ray Tracing Method

Haolin Fan[a], Saiya An[a], Faqin Luo[a]

[a] School of Information and Control Engineering, Qingdao University of Technology, Qingdao, 266525, P. R. China

ARTICLE INFO

Article history:
Received 15 November 2023
Accepted 23 January 2024
Available online 25 January 2024

Keywords:
Monte Carlo Pathing Tracing
Parallel projection method
reflection of rays
concentrating solar power

ABSTRACT

In order to facilitate China's early achievement of the goals of "carbon neutrality" and "peak carbon emissions," the development of new energy-based power systems has become a major research focus. Tower-type solar thermal power generation, as one of the new energy technologies, may be influenced by various optical factors during its construction process. Therefore, to enhance energy utilization efficiency, this study utilized the Monte Carlo ray tracing method to calculate the optical efficiency and output power of a specific circular heliostat field.

1. Introduction

The energy issue in today's world has become increasingly significant. With the contradiction between the growing demand for energy consumption driven by human development and the diminishing existing resources becoming more pronounced. Therefore, it is crucial to establish a new type of power system with renewable energy sources as the primary component.

The construction of tower-type solar thermal power generation, as a new type of green and clean energy technology, requires a significant investment during the setup process. Therefore, the design of relevant device parameters becomes particularly crucial.[1]

The solar power tower plant (SPTP) consists of several subsystems with different functions, mainly including heliostat field, solar collector and Photothermal power generation system. During operation, the rotation axis of the heliostat dynamically adjusts the normal direction of the heliostat based on the sun's position. This adjustment facilitates the concentration of sunlight reflections onto the collector device situated on the absorption tower. Consequently, the internal thermal medium is heated, thereby converting solar light energy into heat energy for storage. Ultimately, this stored heat energy is converted into electricity through the process of heat exchange.

Because the energy conversion efficiency of the device depends on the optical efficiency of the heliostat field, the device will be greatly affected by optical factors in practical work. In order to better reduce the construction cost and improve the energy utilization rate, this paper takes the optical efficiency of the heliostat field as the goal, adopts the ray tracing method based on Monte Carlo to simulate the actual light, calculates the optical efficiency value of the heliostat field, and then obtains the output thermal power, so as to help the subsequent personnel to design the relevant parameters of the heliostat field with higher efficiency.

2. The establishment of heliostat field model

2.1 The establishment of coordinate system

When the heliostat field is in working state, different shadow areas will be generated due to the change of the sun position, thus blocking the mirror reflection function of part of the heliostat, and thus reducing the work efficiency[2].

1) the Heliostat field coordinate system: Therefore, in order to facilitate the calculation of shadow occlusion area and optimize the mirror distribution of heliostat field, this paper takes the tower located in the central region as the origin, The east direction is set as the x axis forward, the y axis forward direction is set as the north direction, and the vertical ground upward direction is set as the z axis forward, and the mirror field coordinate system is established.

2) the Calibration of special symbols: In this paper, based on the coordinate system established above, the center of the collector is $O_a(x_i, y_i, z_i)$, the center of the sun is S, the center of the i heliostat mirror is $O_i(x_i, y_i, z_i)$, the incident light vector is $\overrightarrow{SO_i}$, the

* Corresponding author.
E-mail addresses: haolinfan2002@163.com (H. Fan)
Digital Object Identifiers: https://doi.org/10.62953/IJAMCE.325715

reflected light vector $\overrightarrow{O_iO_a}$, the normal vector line n, and the Angle between the incident light and the normal vector is θ_n .

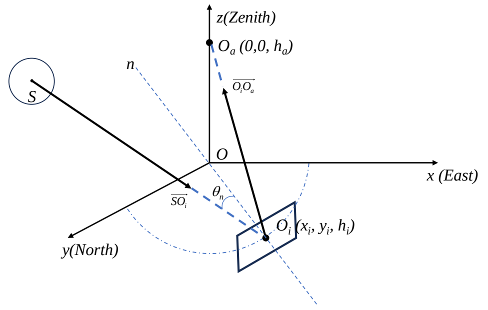

Fig. 1. Heliostat field three-dimensional simplified coordinate system

The heliostat field reflects sunlight onto a receiver for thermal energy storage and thermoelectric conversion operations. Since sunlight forms a fixed cone of light with a specific angular spread, determining the direction of incident light is crucial. To establish the geometric relationship between the solar altitude angle α_s and the solar azimuth angle γ_s .[3]

$$\begin{cases} \sin\alpha_s = \cos\delta\cos\varphi\cos\omega + \sin\delta\sin\omega \\ \cos\gamma_s = \dfrac{\sin\delta - \sin\alpha_s\sin\varphi}{\cos\alpha_s\cos\varphi} \end{cases} \tag{1}$$

where φ respects local latitude, The latitude is positive in the northern hemisphere, and ω represents the hour angle of the sun. ST represents the local time, and δ represents the solar declination angle.

$$\begin{cases} \omega = \dfrac{\pi}{12}(ST-12) \\ \sin\delta = \sin\dfrac{2\pi D}{365}\sin(\dfrac{2\pi}{360}23.45) \end{cases} \tag{2}$$

Where D respects the days are counted starting from the vernal equinox.

This study adopts the observer's location's horizon as the origin of the coordinate system and the *xoy*-plane. The zenith, located at the highest point in the hemisphere, is used as the top of the Earth. A line is drawn from the center perpendicular to reach the zenith, establishing a horizontal coordinate system as shown in Fig. 2. This facilitates geometric analysis of the relevant angles.

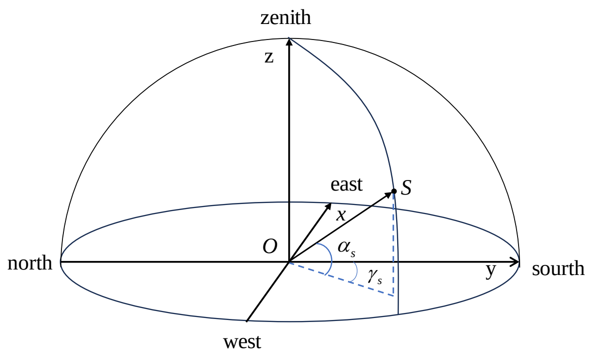

Fig. 2. Horizontal coordinate system

2.2 The Principle of Heliostat Sun-tracking

When analyzing the optical path of heliostat mirrors, it's important to note that sunlight in real life is not parallel but rather forms a cone of light with a certain angular spread.[4]The angular spread of the cone of light ($2\theta_s$) Satisfying the following equation：

$$2\theta_s = \frac{D}{r_s} \tag{1}$$

It is known that the sun-earth distance D is 1.5×10^8 km, and the solar radius r_s is 6.96×10^5 km, which are brought into formula (1), and the conical Angle of the sunlight cone can be obtained as about 9.35mrad, which is converted to 0.533°. In addition, according to the law of light reflection, it can be determined that the Angle of incident and reflected solar rays on the helioscope is 0.533° light cone.

In order to understand the occlusion of the shadow on the Heliostat mirror, this paper selects the center line of the sunlight cone, namely the main incident light, to draw the light path model, so as to analyze the light path of the mirror. Since the movement of the heliostat is determined in real time according to the position of the sun, the main reflected light that always meets the center of the heliostat can be reflected into the center of the collector. Therefore, the main reflected light vector of the heliostat center can be determined according to the heliostat center $O_i(x_i, y_i, z_i)$ and the collector center $O_a(x_i, y_i, z_i)$, which is calculated as follows:

$$\overrightarrow{o_io_a} = \frac{o_i - o_a}{|o_i - o_a|} \tag{3}$$

In the same way, the unit vector $\overrightarrow{SO_i}$ of the main incident light directed from the center of the Sun to the center of the heliostat is calculated by:

$$\overrightarrow{so_i} = \frac{s - o_i}{|s - o_i|} \tag{4}$$

Since the unit normal vector $n(x_n, y_n, z_n)$ of the heliostat represents the orientation of the heliostat, the direction of the vector should be perpendicular to the plane and square the incident reflection vector of the heliostat, its calculation formula is as follows:

$$\vec{n} = \frac{s - o_i}{|s - o_i|} \tag{5}$$

3. Solar Position and Incident Light Calculation

In order to obtain a larger area of light, the heliostat will track the sun in real time during the working process, so that the light emitted from the center of the sun, also called the center line of the sun cone, is reflected to the center of the collector through the center of the heliostat. Therefore, in order to accurately determine the rotation of the heliostat axis, it is very important to determine the position of the sun. Since the position of the sun can be determined by the solar altitude Angle α_s and the solar azimuth Angle γ_s, it can be inferred that if the center line of the centerline sun cone is the incident light, its unit vector $\overrightarrow{SO_i} = (x_s, y_s, z_s)$ is expressed as follows:

$$\begin{cases} x_s = \cos\alpha_s \cos(\gamma_s - \frac{\pi}{2}) \\ y_s = \cos\alpha_s \sin(\gamma_s - \frac{\pi}{2}) \\ z_s = \sin\alpha_s \end{cases} \tag{6}$$

4. Modeling of optical efficiency of heliostat

It can be learned from the article[5] that the optical efficiency of the heliostat field η consists of the following five parts: shadow occlusion efficiency η_{sb}, cosine efficiency η_{cos}, atmospheric transmittance η_{at}, truncation efficiency η_{trunc}, and the mirror reflectance η_{ref}. The specific formula is as follows:

$$\eta = \eta_{sb}\eta_{cos}\eta_{at}\eta_{trunc}\eta_{ref} \tag{7}$$

4.1 Shadow loss caused by absorption tower to heliostat field

The shadow occlusion efficiency η_{sb} is

$$\eta_{sb} = 1 - \textit{Shadow occlusion loss} \tag{8}$$

In the helilostat field, excluding the influence of special weather, it can be determined that the shadow occlusion loss is mainly composed of three parts: ①the shadow effect of the absorber tower on the heliostat field; ②some incident light rays from the rear-row heliostats may be blocked by the front-row heliostats; ③some reflected light rays from the rear-row heliostats may fall onto the back surface of the front-row heliostats. [6] Due to the impact of the shadow occlusion from the absorber tower on the heliostats' sunlight collection, it should be given priority consideration.

In order to calculate the shadow loss caused by the tower, the plane projection method is used in this paper. According to the direction of the incident light ray, the area of the tower projected onto the ground under sunlight is calculated. In this model, since the overall shape of the absorber tower is a cylinder, its projection on the ground under sunlight should be a parallelogram.

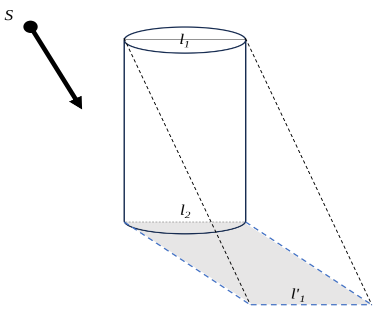

Fig. 3. Projection diagram of the tower

A cross-section is selected within the cylinder corresponding to the absorber tower, such that the cross-section is perpendicular to the incident light ray and its base is the diameter of the bottom circle of the cylinder. By projecting this along the incident light ray onto the ground plane, the projected shape of the absorber tower can be obtained.

During the projection process, considering that the base of the projection plane coincides with the cross-section of the absorber tower itself, it is only necessary to determine the position of the top edge cof the projection plane. Then, connecting each end point of l_1' with l_2' will complete the projection plane, allowing for the calculation of the area of the entire projection plane. In the coordinate system shown in Fig. 1, the shadow occlusion diagram of the tower at different times is calculated through programming, as shown in the Fig. 4.

In addition, due to the working state of the heliostats being planned with their centers facing the target, and considering the large number of heliostats, individually calculating the shadow occlusion situation of each heliostat by the absorber tower would involve significant computation and unpredictable errors. In practical construction processes, the proportion of heliostats affected by shadow occlusion should be relatively small. In order to simplify the calculation, this paper determines whether the reflected light of the heliostat can be directed to the center of the collector according to whether the central coordinate of the heliostat is located in the projection plane of the absorber, and then calculates the proportion of the heliostat area obscured by the shadow of the absorber to the total area.

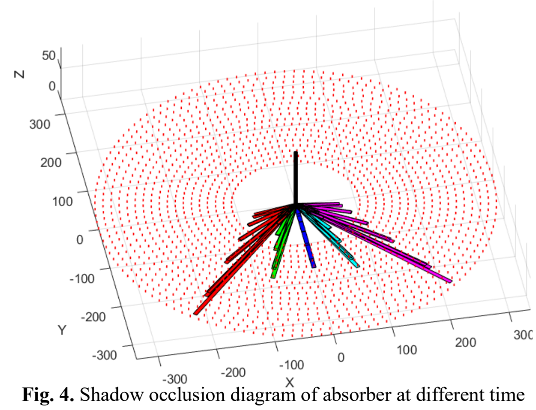

Fig. 4. Shadow occlusion diagram of absorber at different time

The projection chart above illustrates the moments from 9:00 AM to 3:00 PM, with the x-axis indicating time intervals of 9:00, 10:30, 12:00, 13:30, and 15:00 respectively, moving from right to left.

4.2 Modelling the heliostat field optical efficiency

In order to further calculate the shadow blocking efficiency of heliostat field, should first eliminate the completely blocked heliostat at different time points, and only consider the shadow blocking loss between the remaining heliostat.

The Fig. 5 specifically simulates the occlusion loss process of the heliostat, in which part of the main incident light incident to the heliostat A blocks part of the area in the rear heliostat B due to its own attitude. On the other hand, part of the main reflected light reflected on the surface of heliostat B will be occluded by the back of the heliostat A in front, so that it cannot be reflected into the collector, resulting in the corresponding occlusion loss.

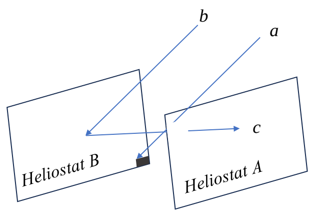

Fig. 5. Simulation of occlusion loss

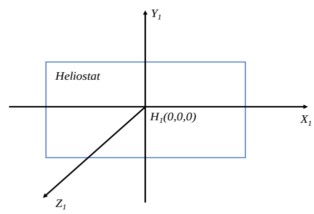

Fig. 6. Mirror coordinate system

Through literature review, it is found that researchers both domestically and internationally have proposed various methods for calculating shadow occlusion efficiency. However, these methods can be primarily categorized into two main approaches based on their principles: Monte Carlo ray tracing method and planar projection method.

Considering the high accuracy of Monte Carlo ray tracing, this paper uses Monte Carlo ray tracing to calculate the occlusion loss.[7]Monte Carlo is a statistical simulation algorithm that uses random numbers to simulate a specific environment. When Monte Carlo is used for ray tracing, it constitutes a probabilistic algorithm for ray tracing. It simulates the lighting effects between objects by iteratively using a large number of random values. The specific algorithmic flowchart for Monte Carlo ray tracing is shown in the Fig. 7.

The specific calculation method of the occlusion loss is to select A point from the heliostat A shown in Fig. 5, extend the main incident light passing through the point in the forward direction and extend the main reflection light in the reverse direction, and determine whether it falls in the mirror surface of the heliostat B, so as to calculate the light blocking area.

Considering that in the Heliostat field coordinate system, it is difficult to directly calculate the coordinate range of different normal vectors of the mirror, and it is difficult to calculate the overlap area. Therefore, the mirror coordinate system as shown in Fig. 6 is introduced in this problem, and the intersection calculation between the vector and the plane in the 3D coordinate system is transformed into the calculation of whether the points on the main incident light and the main reflected light in the 2D plane are located in the heliostats that are occluded by each other, so as to realize the calculation of the shadow occlusion area.

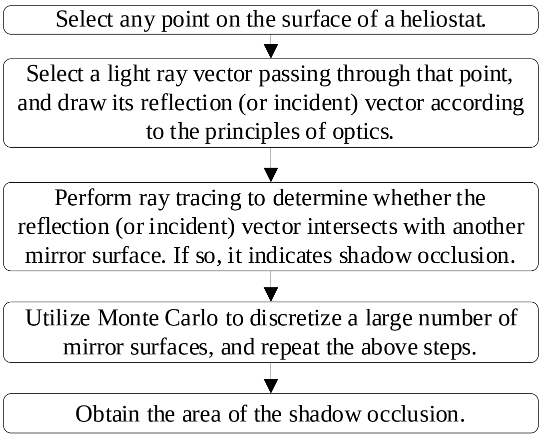

Fig. 7. Shadow occlusion diagram of absorber at different time

The coordinate system takes the width and height of heliostat i as the X_i axis and Y_i axis, and the normal direction perpendicular to it as the Z_i axis, so the plane center coordinate of heliostat i is its origin $H_i(0,0,0)$.

In the mirror A shown in Fig. 5, choose an arbitrary point $H_A(x_1, y_1, 0)$. Arbitrarily select a ray of light passing through HA and extending to intersect with the plane where mirror B is located, with the point on mirror B's coordinate system denoted as $H_B(x_2, y_2, 0)$. By combining the coordinates of H_A with the direction vector of the light ray, construct the equation of the line using the point-direction form. Subsequently, determine the coordinates of the intersection point of this line with the plane where mirror B is located. Finally, ascertain whether this point lies within mirror B, thus delineating the entire shadow region.

In the specific calculation process, considering the difficulty in determining the conversion relationship between different heliostats' angles, an intermediate coordinate system, known as the heliostat field coordinate system, is introduced. Formula derivation is conducted based on the relationship between different mirror coordinate systems and the heliostat field coordinate system. The detailed process is as shown in the Fig. 8.

1) According to the rotational mechanism of the heliostat, we establish the unit rotation matrix (9) to rotate the coordinate axes *x*, *y*, *z* of the mirror coordinate system into the mirror field coordinate system.

$$T=\begin{bmatrix} u_x & u_y & u_z \\ v_x & v_y & v_z \\ w_x & w_y & w_z \end{bmatrix}=\begin{bmatrix} -\sin AH & -\cos AH\cos EH & \cos AH\sin EH \\ \cos AH & -\sin AH\cos EH & \sin AH\sin EH \\ 0 & \sin EH & \cos EH \end{bmatrix} \quad (9)$$

where *EH* and *AH* respectively represents the Pitch Angle and azimuth Angle of heliostat normal. The range is from 0 to 90 degrees and from 0 to 360 degrees, respectively.

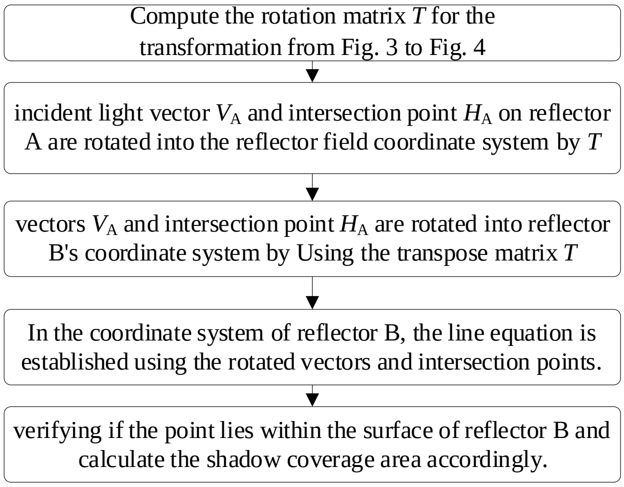

Fig. 8. Calculate occlusion shadow flow chart

2) Assuming the vector representing the light ray in mirror coordinate system A is represented as $\overrightarrow{V_A}$, in mirror coordinate system B is represented as $\overrightarrow{V_B}$, and in mirror field coordinate system as $\overrightarrow{V_O}$, combined with equation (9), the relationship between vector $\overrightarrow{V_A}$ and vector satisfies the following equation:

$$\overrightarrow{V_o}=T\cdot\overrightarrow{V_A} \quad (10)$$

Similarly, utilizing equation (8), the light ray in mirror coordinate system A, represented by $\overrightarrow{V_A}$, and the intersection point $H_A(x_1, y_1, 0)$ on the mirror surface are rotated to obtain coordinates $H'(x_1', y_1', z_1')$ in the mirror field coordinate system.

$$T=\begin{pmatrix} u_x & u_y & u_z \\ v_x & v_y & v_z \\ w_x & w_y & w_z \end{pmatrix}\cdot H_1+o_A=\begin{pmatrix} x_1' \\ y_1' \\ z_1' \end{pmatrix} \quad (11)$$

where o_A represent the coordinates of the center of mirror A in the mirror field coordinate system are denoted as (x_A, y_A, z_A).

3) Connecting the coordinates of $H_A^{'}$ in the mirror field coordinate system with the intersection point of the center of mirrors B. Then rotating it to the mirror coordinate system of mirror B to obtain the corresponding coordinates of point $H_A^{"}(x_1^{"}, y_1^{"}, z_1^{"})$.

$$H_1^{"} = \begin{pmatrix} u_x & u_y & u_z \\ v_x & v_y & v_z \\ w_x & w_y & w_z \end{pmatrix}^T \bullet (H_1^{'} + o_B) = \begin{pmatrix} x_1^{"} \\ y_1^{"} \\ z_1^{"} \end{pmatrix} \tag{12}$$

where o_B represents the coordinates of the center of mirror B in the heliostat field coordinate system.

Similarly, we can transform the light ray vector $\overrightarrow{V_O}$ from the mirror field coordinate system to the mirror coordinate system of mirror B, obtaining the vector $\overrightarrow{V_B} = (x_{B,A}, y_{B,A}, z_{B,A})$.

4) In the mirror coordinate system of mirror B, utilizing vector $\overrightarrow{V_B}$ and the coordinates of point $H_A^{"}(x_1^{"}, y_1^{"}, z_1^{"})$, we establish the beam line equation using the point direction form.

$$\frac{x - x_1^{"}}{x_{B,A}} = \frac{y - y_1^{"}}{y_{B,A}} = \frac{z - z_1^{"}}{z_{B,A}} \tag{13}$$

5) Substituting the point of intersection $H_B(x_2, y_2, 0)$ of the beam line with mirror B into this equation, then calculating the relevant relationships.

$$\begin{cases} x_2 = \dfrac{z_{B,A}x_1^{"} - x_{B,A}z_1^{"}}{z_{B,A}} \\ y_2 = \dfrac{z_{B,A}y_1^{"} - x_{B,A}z_1^{"}}{z_{B,A}} \end{cases} \tag{14}$$

By verifying if point H_B falls within the mirror surface of mirror B, to infer shadow occlusion between heliostats, and calculate the shadow occlusion area. Adding it to the absorber tower's shadow occlusion area to determine the total shadow occlusion area, thereby computing the shadow occlusion efficiency.

$$\eta_{sb} = \frac{S_A + S_{sb}}{S_z} \tag{15}$$

where S_A represents the shadow occlusion area generated by the absorber tower, S_{sb} represents the shadow occlusion loss area between heliostats, S_Z represents the total heliostat field illuminated area.

4.3 Theoretical Model of Truncation Efficiency

The truncation efficiency η_{trunc} of the collector refers to the percentage of energy it receives compared to the total energy concentrated in the heliostat field. Here, the energy concentrated in the heliostat field refers to the energy reflected by the mirrors, accounting for shadow occlusion and energy attenuation.

Because the outermost heliostats in the heliostat field are farthest from the central tower, while the innermost ones are closest. Considering that both incident and reflected sunlight consist of a cone of light with a certain cone angle, and the farther the distance, the larger the cross-section of the light cone. Therefore, the sizes of the reflection spots on the central receiver tower vary for different heliostats, leading to some heliostats' reflection spots not completely covering the receiver, thus resulting in truncation losses.

To calculate the truncation loss of heliostats, we first need to compute the proportion of the ineffective area on the collector surface covered by each heliostat's reflected beam spot to the total area. Since the plane normal of the heliostat is determined by the simultaneous solution of the primary incident ray and the primary reflected ray, separate calculations are needed for the reflection direction of the remaining rays within the beam.

To compute the direction of all reflected rays, the incident rays are discretized first. Using angular subdivision, a beam of light is divided into several rays, as illustrated in the diagram. Then, employing the law of reflection, the reflection direction for each ray is calculated. Subsequently, the proportion of rays entering the collector to the total number of rays is determined, thereby computing the collector's truncation efficiency η_{trunc}.

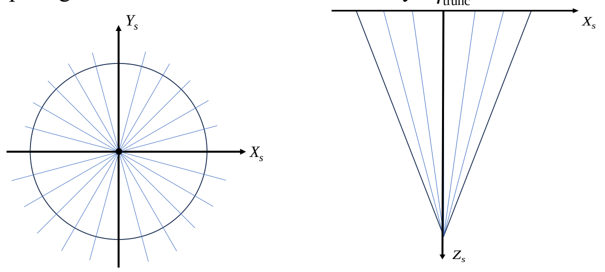

Fig. 9. Angular subdivision method divides the beam of light equally

For ease of calculating the number of effective rays in each reflected light cone, the z_S axis is initially aligned with the primary incident ray, directed towards the center of the solar disk. Then, the x_S axis is established parallel to the x-axis of the mirror field coordinate system within the beam. Finally, the y_S axis is set up perpendicular to the $x_s o z_S$ plane.

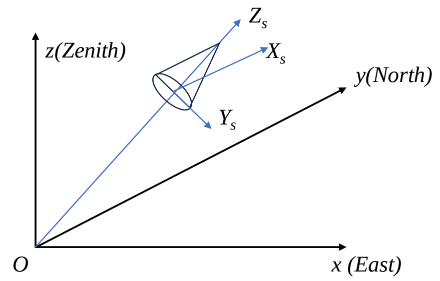

Fig. 10. The light cone coordinate system

Given the unit direction vector of the primary incident light ray, other light rays can be determined based on their angles σ with the primary incident light ray and angles τ with the X_s axis. Each vector of light ray within the light cone satisfies

$$\overrightarrow{S_s} = (\sin\sigma\cos\tau, \sin\sigma\sin\tau, \cos\sigma) \tag{16}$$

In this question, we first select a vector representing a light ray, denoted as $\overrightarrow{V_s} = (a, b, c)$ in the light cone coordinate system. To determine whether its reflected light ray will intersect with the outer surface of the collector, we need to construct the straight line equation through which this vector passes. Therefore, we need to select another point related to this light ray vector. We can refer to the process of solving the shadowing efficiency to select the intersection point of the incident light ray with Mirror A, denoted as H_{A}, with its coordinates in the mirror field coordinate system as $H_{\mathrm{A}}^{'}(x_1, y_1, 0)$. The specific solution process of the truncation efficiency η_{trunc} is as shown in the Fig. 11.

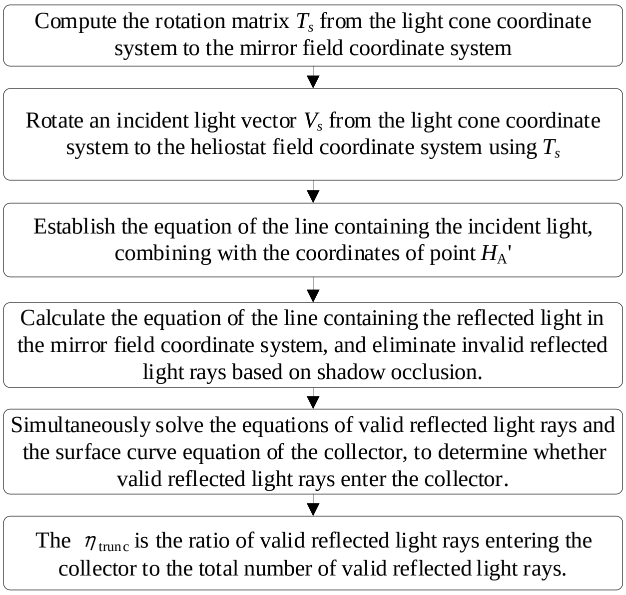

Fig. 11. Truncation efficiency η_{trunc} solving process diagram

1) Considering the solar altitude and azimuth angles, calculate the rotation matrix T_s from the light cone coordinate system to the mirror field coordinate system.

$$T_s = \begin{pmatrix} \sin\gamma_s & -\sin\alpha_s\cos\gamma_s & \cos\alpha_s\cos\gamma_s \\ -\cos\gamma_s & -\sin\alpha_s\sin\gamma_s & \cos\alpha_s\sin\gamma_s \\ 0 & \cos\alpha_s & \sin\alpha_s \end{pmatrix} \tag{17}$$

Rotate the light ray vector $\overrightarrow{V_S}$ from the light cone coordinate system to the mirror field coordinate system.

$$\overrightarrow{V_{SG}} = T \cdot \overrightarrow{V_S} = (a_1, b_1, c_1) \tag{18}$$

2) From Fig. 1, it can be observed that in the mirror field coordinate system, the reflection vector $\overrightarrow{V_{SR}}$ corresponding to the incident light vector $\overrightarrow{V_{SG}}$ can be calculated based on the normal vector of the mirror $\overrightarrow{V_N}$. The specific process is as follows

$$\begin{cases} \cos\theta = \overrightarrow{V_{SG}} \cdot \overrightarrow{V_N} \\ \overrightarrow{V_{SG}} = 2\cos\theta\overrightarrow{V_N} - \overrightarrow{V_{SR}} = (m, n, l) \end{cases} \tag{19}$$

3) Determine the intersection point of the reflected light ray with the collector surface.

$$\begin{cases} \dfrac{x - x_1^{'}}{m} = \dfrac{y - y_1^{'}}{n} = \dfrac{z - z_1^{'}}{l} \\ x^2 + y^2 - R^2 = z \end{cases} \tag{20}$$

Where R and z respectively represents the collector radius and height. 4) Filter out the valid reflected light rays entering the collector, and calculate the truncation efficiency η_{trunc}.

$$\eta_{\mathrm{trunc}} = \frac{W_{\mathrm{a}}}{W_{TF} - W_{\mathrm{ab}}} = \frac{C_{RA}}{C_R} \tag{21}$$

Where W_{a} represents the energy received by the collector, W_{TF} denotes the energy from total internal reflection on the mirror surfaces, and W_{SB} signifies the energy loss due to shadowing and blocking.

4.4 Theoretical model of optical efficiency

Cosine efficiency $\eta_{\cos}$ is

$$\eta_{\cos} = \cos\theta_{\mathrm{n}} \tag{22}$$

Where θ_{n} respects the angle between the incident light vector and the mirror surface normal.

Atmospheric transmissivity η_{at} is

$$\eta_{\mathrm{at}} = 0.99321 - 0.0001176 d_{HR} + 1.97 \times 10^{-8} \times d_{HR}^2 \tag{23}$$

Where d_{HR} respects the distance from each mirror center to the collector center.[8]

Truncation efficiency η_{trunc} refers to the impact of atmospheric attenuation on the solar radiation reflected from the heliostats to the receiver, resulting in radiation loss. The specific equation as follows:

$$\eta_{\mathrm{trunc}} = \frac{\text{Energy received by the collector}}{\text{Total reflection energy Shadow occlusion loss energy}} \tag{24}$$

The reflectance of the mirror surface η_{ref} can be assumed to be constant, such as 0.92.

4. The thermal power output of the heliostat field

In the preceding sections, the calculation process for the optical efficiency of heliostats has been thoroughly discussed. To assess the effectiveness of the heliostat field layout, it is essential to compute the thermal power output of the heliostat field E_{field}. Therefore, the optical efficiency η will be incorporated into the formula (25) for calculating the thermal power output of the heliostat field.

$$E_{\mathrm{field}} = \mathrm{DNI} \cdot \sum_{i}^{N} A_i \eta_i \tag{25}$$

Where DNI respects the Direct Normal Irradiance. N respects the total number of heliostats. A_i respects the heliostat area for the i^{th} heliostat. η_i respects the optical efficiency η for the i^{th} heliostat.

Direct Normal Irradiance (DNI) respects the solar irradiance, or insolation, on a unit area perpendicular to the Sun's rays at the Earth's surface, received in unit time, can be approximated by the following formula:

$$\begin{cases} \mathrm{DNI} = G_0[a + b \cdot \exp(-\dfrac{c}{\sin\alpha_s})] \\ a = 0.4237 - 0.00821(6 - H)^2 \\ b = 0.5055 + 0.00595(6.5 - H)^2 \\ c = 0.2711 + 0.01858(2.5 - H)^2 \end{cases} \tag{26}$$

Where G_0 respects the solar constant, which refers to the average amount of solar radiation received per unit area at a distance of one astronomical unit (AU) from the Sun. It is approximately 1361 watts per square meter[9].

5. Results

The data for this study is derived from Problem A of the 2023

Mathematical Modeling National Competition. It is anticipated that a circular solar field will be constructed within a circular area with a radius of 350 meters, centered at approximately 98.5° east longitude and 39.4° north latitude, at an elevation of 3000 meters above sea level, as illustrated in the diagram below.

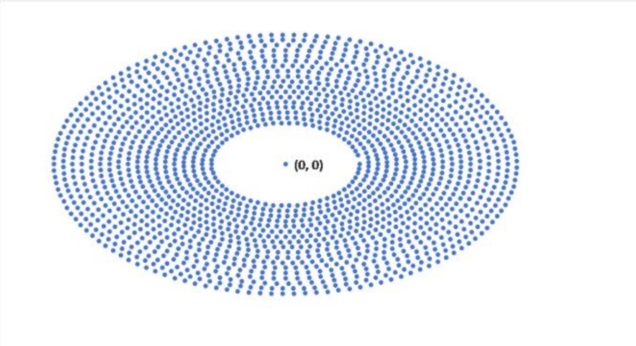

Fig. 12. The distribution map of heliostats

In the planned layout, the receiver tower has a height of 80 m, and the collector is a cylindrical external surface receiver with a height of 8 m and a diameter of 7 m. No heliostats are installed within a range of 100 m around the receiver tower to provide space for constructing buildings for installing power generation, energy storage, control, and other equipment. The heliostats are rectangular in shape, with both the upper and lower edges parallel to the ground. The dimensions are 6 m × 6 m, and the installation height is 4 m.

In calculating shadow occlusion efficiency and truncation efficiency, this study employs the Monte Carlo ray tracing method, which accurately computes the optical path of each ray, thereby enhancing the accuracy of the results. But, due to the necessity of discretizing a large amount of data during Monte Carlo ray tracing analysis, the model-solving process is time-consuming.

On the other hand, in calculating shadow loss, this study employs a binary approach to determine if the entire mirror surface is covered by the shadow of the absorber tower. Although the proportion of mirror surfaces affected by the absorber tower is small, there may still be some errors. However, by fluctuating the calculated shadow occlusion area by 10%, the variation in output thermal power of the heliostat field is obtained as shown in the table below.

Tab. 1. Sensitivity of shadow loss

Changes in loss	90% of shadow loss	110% of shadow loss
Rate of change in thermal power output of the heliostat field	0.003076573	0.003083673

Similarly, in calculating truncation efficiency, due to the use of Monte Carlo ray tracing method, the specific sampling has a certain randomness. Therefore, using the same method, sensitivity analysis of the collector truncation efficiency is conducted by adjusting the number of valid reflected rays falling into the collector.

Tab. 2. Sensitivity of Truncation loss

Changes in loss	90% of truncation loss	110% of truncation loss
Rate of change in thermal power output of the heliostat field	0.005462023	0.005462023

From the Tab.1 and Tab.2, it can be observed that even if there are discrepancies in the calculation of shadow occlusion area and the number of valid reflected rays falling into the collector, the impacts on the results are minimal. This further validates the rationalities of the shadow occlusion loss calculation model and truncation efficiency model in this study.

References

[1] Farges O, Bézian J, Hafi E M. Global optimization of solar power tower systems using a Monte Carlo algorithm: Application to a redesign of the PS10 solar thermal power plant[J]. Renewable Energy,2018,119

[2] X. Chen and Z. Chen, "Optimal Design of Heliostat Field," 2023 3rd International Conference on New Energy and Power Engineering (ICNEPE), Huzhou, China, 2023, pp. 327-331.

[3] X.L. Cheng. Study on the Optimal Design of Heliostat Field Layout for Solar Power Tower Plant. Hefei University of Technology, 2018.

[4] O. Farges, J. Bezian, H. Bru, M.E. Hafi, R. Fournier, C. Spiesser, Life-time integration, using Monte Carlo Methods when optimizing the design of concentrated solar power plants, Solar Energy. solener. 2014. 12. 027.

[5] M. Zhang, L. Yang, C. Xu, X. Du, An efficient code to optimize the heliostat field and comparisons between the biomimetic spiral and staggered layout, Renew. Energy. ISSN: 0960-1481 87 (2016) 720e730

[6] R.T. Wang, X.D. Wei. Analysis on Optical Performance of the Concentrator Field in the Solar Tower Thermal Power System. Acta Photonica Sinica, vol. 37, 2018. A Ray Tracing Method for Calculating the Optical Efficiency of Heliostat Field

[7] J. de La Torre, G. Baud, J. Bezian, S. Blanco, C. Caliot, J. Cornet, C. Coustet, J. Dauchet, M.E. Hafi, V. Eymet, R. Fournier, J. Gautrais, O. Gourmel, D. Joseph, N. Meilhac, A. Pajot, M. Paulin, P. Perez, B. Piaud, M. Roger, J. Rolland, F. Veynandt, S. Weitz, Monte Carlo advances and concentrated solar applications, Sol. Energy. ISSN: 0038-092X 103 (2014) 653e681

[8] M. Schmitz, P. Schwarzbozl, R. Buck, R. Pitz-Paal, Assessment of the potential improvement due to multiple apertures in central receiver systems with secondary concentrators, Sol. Energy 80 (1) (2006) 111e120.

[9] Leary P L, Hankins J D. User's guide for MIRVAL: a computer code for comparing designs of heliostat-receiver optics for central receiver solar power plants [R]. Technical Report, No. SAND77-82801979.

[10] Wang, Y., et al., Research on Robot Path Planning based on Grid Model and Improved Ant Colony Algorithm. International Journal of Applied Mathematics in Control Engineering, 2018. 1(2): p. 143-148.

Haolin Fan is currently pursuing his undergraduate study at Qingdao University of Technology, majoring in automation.

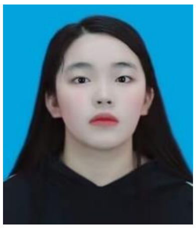

Saiya An is currently pursuing her undergraduate study at Qingdao University of Technology, majoring in Software Engineering.

Faqin Luo is currently pursuing her undergraduate study at Qingdao University of Technology, majoring in Software Engineering.